Journal of Seismology **1:** 15–28, 1997.

Microseismicity, tectonics and seismic potential in southern Caribbean and northern Venezuela

Omar J. Pérez, Carlos Sanz & Gabriela Lagos
Simón Bolívar University, Department of Earth Sciences, Sartenejas, P.O. Box 89.000, Caracas 108, Venezuela

Received 18 June 1996; accepted in revised form 14 March 1997

Abstract

Approximately one thousand microearthquakes with body-wave magnitude m_b have been located in northern Venezuela and the southern Caribbean region (9–12 ° N; 64–70° W) since the installation in 1980 of the Venezuelan Seismological Array, together with forty events of $m_b \leq 4$, one of them with surface-wave magnitude $M_s \sim 6$. Focal depths are in the range of 0 to <15 km. This geologically complex region is part of the boundary between the Caribbean and the South American Plates. Epicentral locations indicate that this E–W oriented portion of the boundary is formed by two ∼ 400 km long subparallel fault zones: San Sebastián fault zone (SSF), ∼ 20 km north of Caracas along the coast; and La Victoria fault zone (LVF), ∼ 25 km south of the city. They are clearly delineated by the microseismicity. New composite focal mechanism solutions (CFMS) along these faults show right-lateral strike-slip (RLSS) motion on nearly E–W oriented fault planes. NW-striking subsidiary active faults occur in the region and intercept the two main E–W fault zones. These interceptions show high levels of microearthquake activity and seismic moment release when compared to other portions of both, the main and subsidiary faults. New CFMS at those fault crossing sites show NW-striking RLSS motion and normal faulting, in an en-echelon-like structural behavior. Geological data and quantitative comparisons with other transcurrent plate boundaries in the world suggest that the rate of plate motion in this area is on the order of 20 mm/y. Several moderate and large shocks have occurred along the SSF and LVF since ∼ 1640, including an $M_s \sim 7.6$ event in 1900 on SSF. Although the region may be relatively far from a repeat of this earthquake, seismicity data indicate that strong shocks could take place along segments of the seismically active faults identified in this study.

Introduction

The purpose of this paper is to analyze the tectonics and seismic potential of southern Caribbean and northern Venezuela (9–12° N; 64–70° W], using an entirely new and revised microseismicity data set gathered by the Venezuelan National Seismological Network, operated by the Venezuelan Foundation for Seismological Research FUNVISIS, for the period 1980 to mid-1995. This region (Figure 1) is part of the E–W oriented boundary between the Caribbean and the South American Plates (e.g., Sykes and Ewing, 1965; Molnar and Sykes, 1969; Jordan, 1975; Burke et al., 1984). The Caribbean plate moves easterly with respect to the South American plate, at a rate of ∼ 20 mm/y or more (Jordan, 1975; Minster and Jordan, 1978; Dewey and Suárez, 1991; Deng and Sykes, 1995).

The central portion of the Caribbean-South American plate boundary (Figure 1) is simpler than that to the west, where it appears to be a multibranched boundary (Dewey and Suárez, 1991; Deng and Sykes, 1995; Pérez et al., 1997). It is also simpler than the boundary to the east, where a NW-dipping slab of Atlantic floor is subducting beneath the Caribbean in the Trinidad region, accompanied by right-lateral strike-slip motion (RLSS) along the E–W oriented El Pilar Fault zone in northeastern Venezuela, and internal deformation in northeastern Venezuela and Trinidad (Pérez and Aggarwal, 1981; Russo et al., 1993). Still, the tectonic fabric in north-central Venezuela exhibits a complex faulting pattern (Figure 2) that includes the

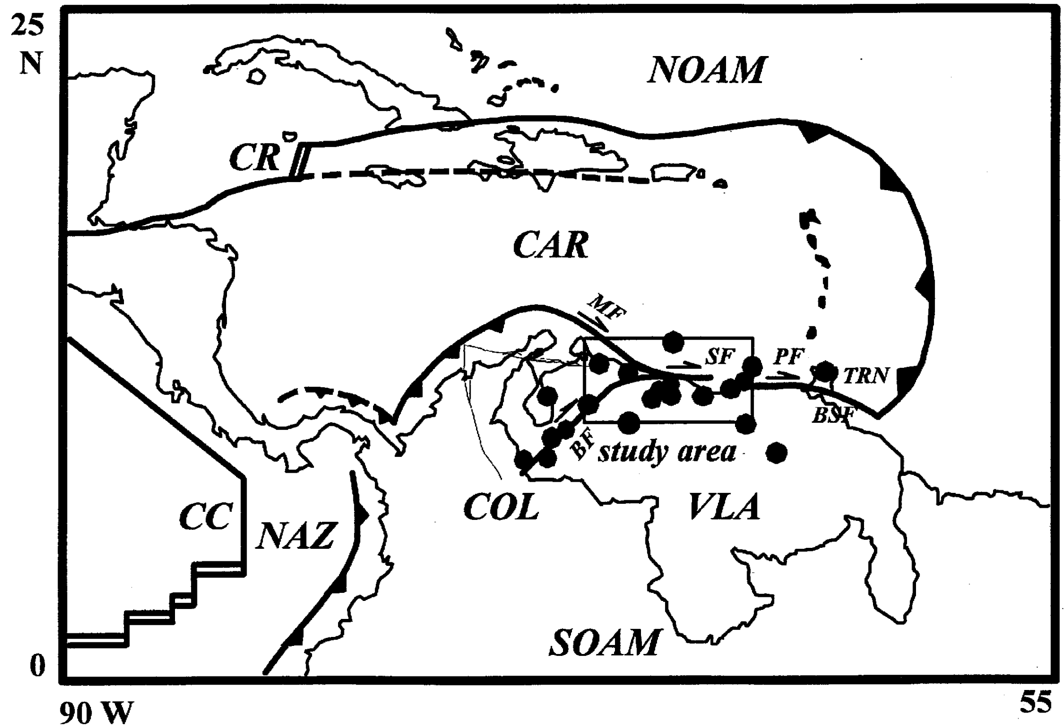

Figure 1. Study area and tectonic setting of Caribbean and adjacent lithospheric plates (modified after Dewey and Suárez (1991) and Pérez et al. (1997)). Main plate boundaries are shown by single or double lines. Dashed lines denote uncertain boundaries. Segments with teeth indicate subduction with teeth on overthrust plate. CR: Mid-Cayman Rise. Plates, CAR: Caribbean; NOAM: North American; CC: Cocos; NAZ: Nazca; SOAM: South American. VLA: Venezuela; COL: Colombia; TRN: Trinidad. BF, MF, SF, PF and SBF are major fault zones in Venezuela: Boconó, Morrocoy, San Sebastián, El Pilar and El Soldado-Los Bajos, respectively. Solid circles represent short-period, single-component seismological stations belonging to the Venezuelan National Seismological Array. Arrows indicate general sense of motion along major faults in Venezuela. Inset shows the location of Figures 2, 3, 4, 8 and 9.

E–W-oriented RLSS San Sebastián and La Victoria fault zones (Rod, 1956; Bellizzia, et al. 1976; Schubert, 1981; Beltrán, 1993); as well as a series of faults oriented in a NW–SE direction. Moreover, the role played by each one of these faults in accommodating the relative motion between the Caribbean and the South American plates is not well known, and thus it has been difficult to evaluate the seismic potential of the region.

This lack of knowledge stems in part from the scarcity of seismological data for the area, which has a relatively low background earthquake activity when compared to other regions in the country and the world (e.g., Fielder, 1961; Suárez and Nabelek, 1990). Indeed, only one large shock, with a corrected surface-wave magnitude $M_s \sim 7.6$ (Pérez and Scholz, 1984; Pacheco and Sykes, 1992) has occurred in the region this century (October 29th, 1900), rupturing large portions of San Sebastián fault (Fielder, 1961; Kelleher et al., 1973; Y. P. Aggarwal, unpublished data, 1987). However, moderate events (e.g., on July 29th, 1967, $M_s = 6.5$; April 10th, 1989, $M_s = 6.0$; see Figure 2) have caused strong damage to several towns, particularly to Caracas in 1967, with a toll of more than 200 deaths and over US $500 million in damage.

In this paper, using precisely located microearthquakes that occurred from 1980 to mid-1995, newly determined composite fault plane solutions, an analysis of historical and teleseismic data, and geological evidence, we show that in this region the Caribbean-South America plate boundary is mainly formed by two ~ 400 km long, E–W-oriented RLSS subparallel fault zones: San Sebastián fault zone (SSF), ~ 20 km north of Caracas along the coast; and La Victoria fault (LVF), ~ 25 km south of the city. In our interpretation, the main plate boundary – that is, the fault zone along which most of the Caribbean-South American motion is released during great earthquakes – is the SSF zone.

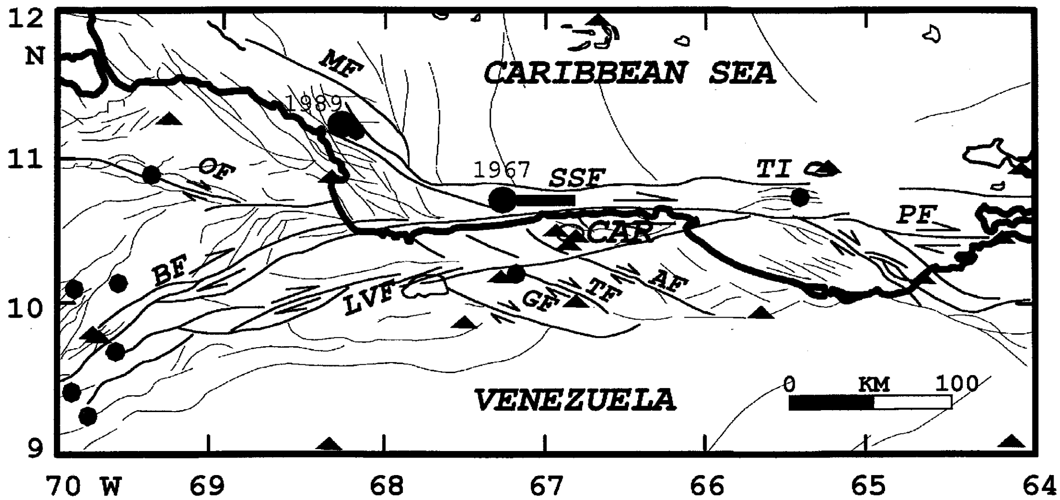

Figure 2. Faults with activity during Quaternary times in north-central Venezuela (from Beltrán, 1993). Faults names as follows: BF: Boconó, MF: Morrocoy, OF: Oca, LVF: La Victoria, SSF: San Sebastián, GF: Río Guárico, TF: Tácata, AF: Araguita, PF: El Pilar. Arrows indicate sense of motion. TI: Tortuga Island. CAR: Caracas. Closed triangles indicate short-period, single component seismological stations belonging to the Venezuelan National Seismological Array. Circles are events with body wave magnitude $m_b \geq 5$ from 1965 to 1995, located by the World Wide Standardized Seismological Network – WWSSN –. Larger circles correspond to events with surface wave magnitude $M_s \geq 6$ in 1967 and 1989. Thick line adjacent to the 1967 main epicenter indicates the extend of its rupture zone (Suárez and Nábêlek, 1990).

Our observations indicate, however, that moderate and large earthquakes have also taken place along LVF, contributing significantly to the motion between the two plates. We also show that NW–SE striking, seismically active faults occur in the region and intercept the two main E–W-oriented fault zones. New composite focal mechanism solutions (CFMS) at these fault crossing sites show a combination of NW striking RLSS motion and normal faulting, in an en-echelon-like structural behavior. On the basis of the historical seismicity and seismotectonic interpretations, we also conclude that although the region may be relatively far from a repeat of the 1900 shock, strong earthquakes could occur along segments of the seismically active faults identified by means of the microseismicity data.

First we present the new microseismicity data set. Then we show our seismotectonic interpretations and an analysis of the historical seismicity of the region. Based on these observations and interpretations, we evaluate the seismic potential of the region under investigation.

Microseismicity data analysis

Figure 3 shows the spatial distribution of microearthquakes (circles) with body-wave magnitude $m_b \geq 2.5$ located in north-central Venezuela, obtained by the Venezuelan National Seismological Array from 1980 to mid-1995. The seismological station sites are shown in Figures 1 and 2. All events located in the region have focal depths $h<20$ km. A cut-off magnitude of $m_b = 2.5$ is used in this map because earthquake locations are more precise for this magnitude range, due to the fact that these shocks are typically well recorded at four to six (or more) nearby seismological stations; and because our initial aim is to find faults showing earthquake activity. This was a primary reason for installing the Venezuelan Seismological Array in 1980. We should point out that we relocated most of the events reported in the FUNVISIS earthquake catalogs, including those corresponding to three surges of seismic activity in 1986, 1989 and 1990, associated with events with $m_b \geq 5$ east of $\sim 69°$ W (Figure 2), and with an earthquake swarm in 1995 that took place around 10.2° N, 67.8° W, at the interception of the Río Guárico (GF) and La Victoria (LV) faults.

Composite focal mechanism solutions were obtained for several groups of events in the region (Figure 4). They are shown in lower hemisphere, equal area projections, with dark areas indicating the compressional quadrants. The corresponding fault plane parameters are given in Table 1. The detailed solutions for mechanisms numbers 1 to 7 in Figure 4 are shown

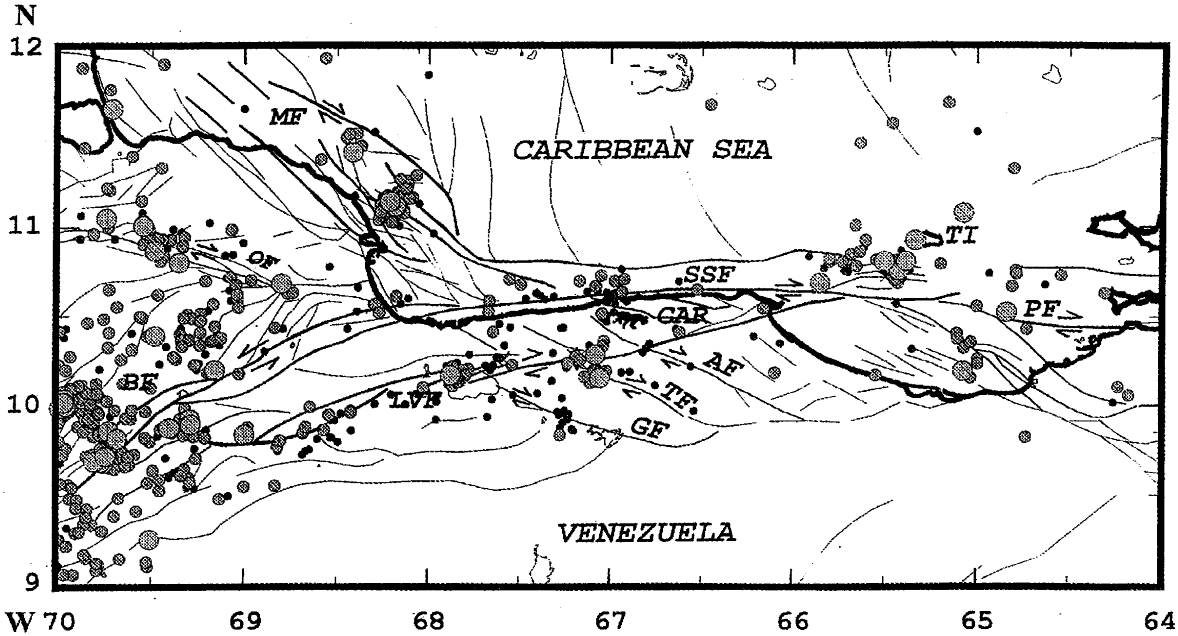

Figure 3. Epicentral distribution of seismicity (circles) located by the Venezuelan National Seismological Array from 1980 to mid-1995. The small-size circles indicate events with body-wave magnitudes m_b in the range $2.5 \leq m_b < 3$; medium-size circles are events in the range $3 \leq m_b < 4$; large circles are events with $m_b \geq 4$. Other symbols as in Figure 2. Note the alignment of earthquake activity along La Victoria (LVF) and San Sebastián Fault zones (SSF) in north-central Venezuela.

Table 1. Focal mechanism parameters

						Plane 1		Plane 2		P axis	T axis	ref
Event	date	Lat (°N)	Long (°W)	h (km)	mb	S	D	S	D	Tr°/Pl○	Tr°/Pl°	
1	1985,87,94	10.7	67.0	<15	3 to 3.9	N5°W	60°ENE	N85°E	90°	314/21	216/21	1
2	1990	10.8	65.5	<15	3 to 5.8	N81°E	70°SW	N9°W	90°	304/14	38/14	1
3	1985,87,90	9.9	68.7	<15	3 to 3.9	N12°W	84°SW	N78°E	90°	123/04	33/04	1
4	1995	10.2	67.9	<15	3 to 4+	N-S	80°E	E87°EW	74°N	224/19	133/5	1
5	Sep/94	10.2	67.9	<15	3 to 4	N58°E	68°SE	N22°W	67°SW	109/01	18/33	1
6	1986	10.2	67.0	<15	3 to 5.8	N48°E	65°SE	N39°W	84°SW	07/22	272/13	1
7	1988,89,90	10.3	67.0	<15	3 to 4	N39°W	75°SW	N42°E	60°SE	05/33	267/10	1
8	1986	9.50	69.2	<20	3 to 4+	N45°E	90°	N45°W	60°NE	274/21	176/21	2
9	Apr/89	11.2	68.2	<15	3 to 5.8	N45°W	65°SW	N45°W	81°SE	359/24	98/11	2

1. Composite mechanisms, this study; 2. Pérez et al., [1997]. S: strike; D: Dip; Tr: Trend; Pl: Plunge

in Figures 5 and 6. Mechanisms 8 and 9 are reported elsewhere (Pérez et al., 1997).

Most of the shocks shown in Figure 3 are located within the seismological array. In general, uncertainties in epicentral locations and focal depths can be conservatively estimated as much less than 10 km (J. Mendoza, personal communication, 1995). The crustal and upper mantle structure used by FUNVISIS and in this study is similar to the one derived for the Venezuelan region by Pérez and Aggarwal (1981). Hypocentral locations show insignificant variations when somewhat different crustal structures are used. All relocations were done using an improved version (J. Mendoza, unpublished data, 1995) of the single event location program of Mendoza and Morgan (1985). The techniques we used to relocate the events, as well as to obtain the composite mechanism solutions and to

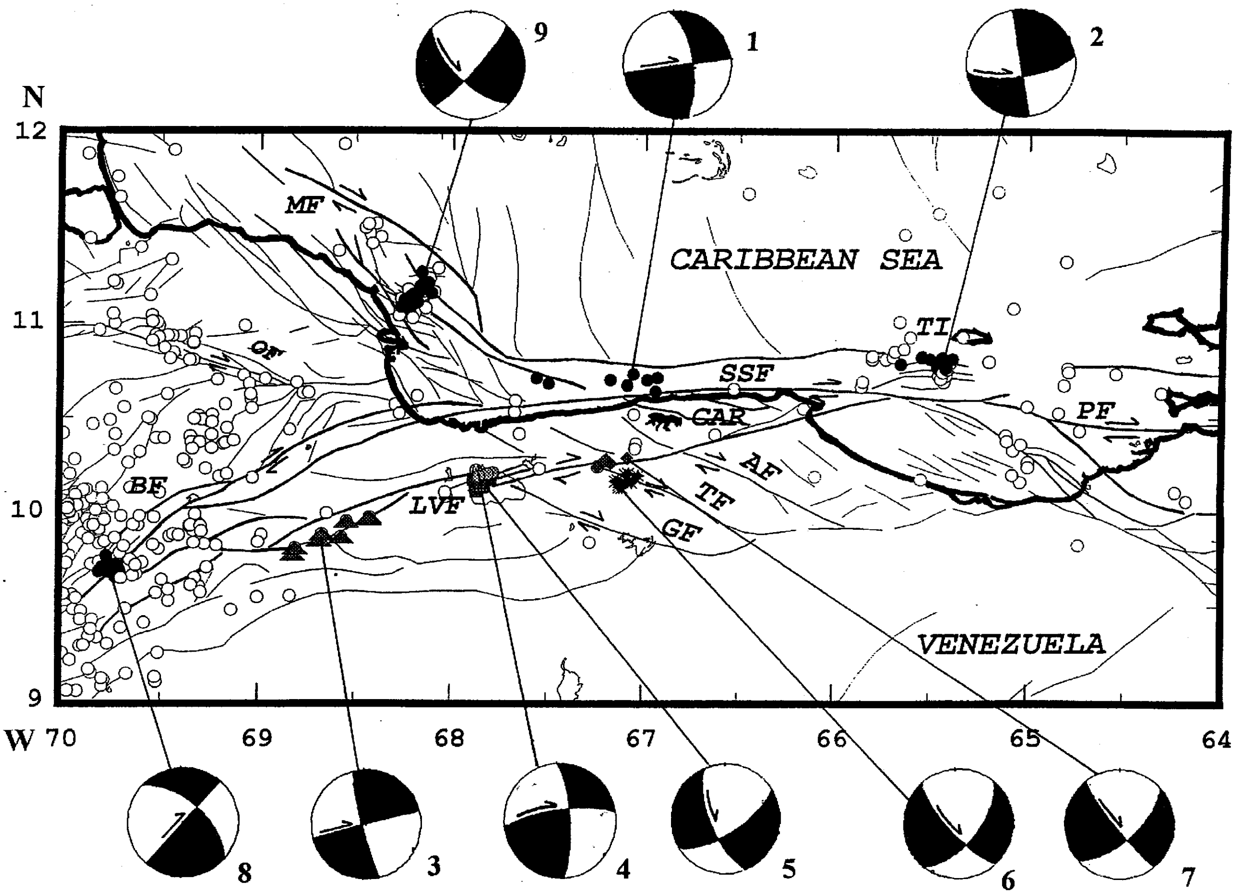

Figure 4. Composite focal mechanism solutions (lower hemisphere, equal area projections; dark areas are the compressional quadrants) for several groups of seismic events (solid symbols), obtained for north-central Venezuela. Numerals are keyed to Figures 5 and 6 and Table 1, where the corresponding parameters are listed. Mechanisms 1 to 7 are new and their detailed solutions are given in Figures 5 and 6. Solutions 8 and 9 are from Pérez et al. (1997). Arrows indicate sense of motion on selected fault planes, as discussed in the text. Events denoted by open circles were not used in any of the nine solutions. All epicenters (solid and open symbols) correspond to earthquakes with $m_b \geq 3$. Other symbols as in Figure 2.

check the quality of the data, are described in detail in a separate paper (Pérez et al., 1997).

Results

Figure 3 displays the spatial distribution of earthquakes (circles; $m_b \geq 2.5$) located in the study area from 1980 to mid-1995. All events have focal depths, h<20 km. Solid lines indicate the traces of major faults occurring in the region (Bellizzia et al., 1976; Beltrán, 1993), that show activity during Quaternary times (Beltrán, 1993). As indicated in Figure 1, the region under investigation is located between the NE-trending Boconó fault zone and NW-oriented Morrocoy fault (BF and MF in Figures 1 to 3, respectively), west of $\sim 69°$ W; and the E–W striking El Pilar fault zone (PF) east of $\sim 65°$ W. Seismotectonic studies of these RLSS fault systems are reported elsewhere (e.g., Pérez and Aggarwal, 1981; Russo et al., 1993; Pérez et al., 1997). Thus, in this paper we will concentrate most of our work in the region between longitudes 65 an d69° W.

Epicentral locations in this area (Figure 3) define a $\sim$400 km long, $\sim$70 km wide, easterly oriented belt of seismic activity. At first glance, this activity may be divided into two subparallel branches: one aligned along the San Sebastián fault zone (SSF) on the coast; and another one straddling La Victoria fault zone (LVF) inland. Earthquake activity also occurs on NW-oriented faults however, namely Río Guárico (GF),

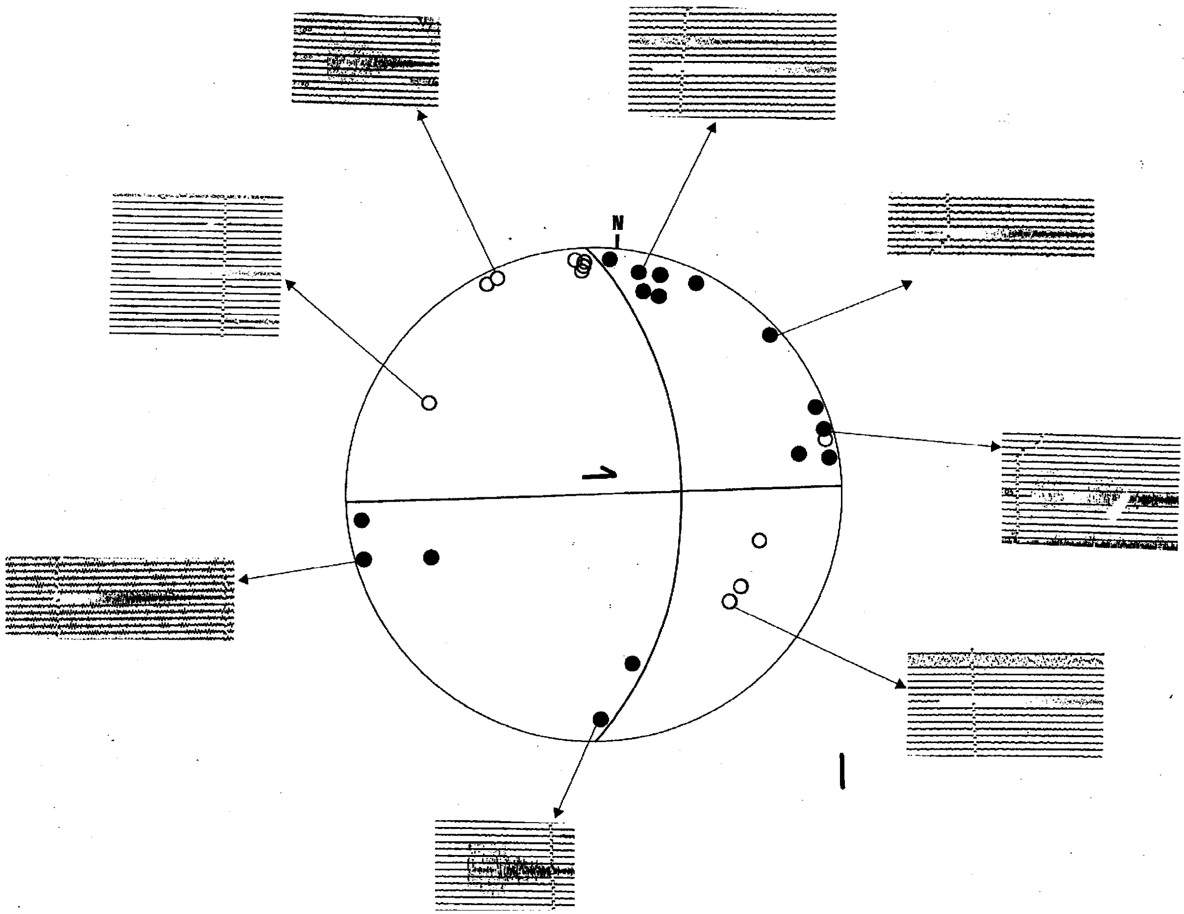

Figure 5. Composite focal mechanism solution (lower hemisphere, equal area projection) for group of events no. 1 in Figure 4 and Table 1. Solid circles are compressions, and open circles are dilatations. *P*-axis (pressure), *T*-axis (tension), and the relative sense of motion (arrows) along the chosen fault plane are indicated. Seismograms show the high quality of the seismic signals generally used in this investigation.

Araguita (AF) and Tácata (TF) faults. We also note that LVF is clearly delineated by the microseismicity from the region SW of La Tortuga Island (TI), down to the Boconó fault zone (BF) in the west, near 9.5°N, 69.5°W, actually intercepting it. This fact was previously unknown from surface geology (A. Bellizzia, personal communication, 1995). We finally note in Figure 3 that although portions of the SSF show no microearthquake activity during the 15 year time-span analyzed, this fault zone along the coast is still well delineated by the microseismicity between its interception with the main traces of the Boconó and Morrocoy faults, in the west, and the region south of TI. In this latter region both, SSF and LVF terminate against a series of NW-oriented RLSS faults (Bellizzia et al., 1976; Beltrán, 1993). Considering the SSF, LVF and PF to the east, as forming the easterly oriented Caribbean–South American plate boundary in the region (as will be discussed in a later section), then what occurs south of TI is a right-stepping offset along the plate boundary itself (Pérez and Aggarwal, 1981).

In an attempt to seek more definitive correlations of earthquakes with faults, we divided the epicenters of events with $m_b \geq 3$ into several groups (Figure 4). The division was done on the basis of either a spatial correlation of epicenters with fault traces, or because the events are located at fault crossing sites. For each group we determined composite focal mechanisms using only unambiguous *P*-wave first motion data (Figures 4, 5 and 6), and constructed vertical profiles of focal depth distribution (Figure 7). A cut-off magnitude of $m_b = 3$ was used to get fault plane solutions, so that only high quality data are used in our interpretations. Different symbols and numerals are used for different groups in

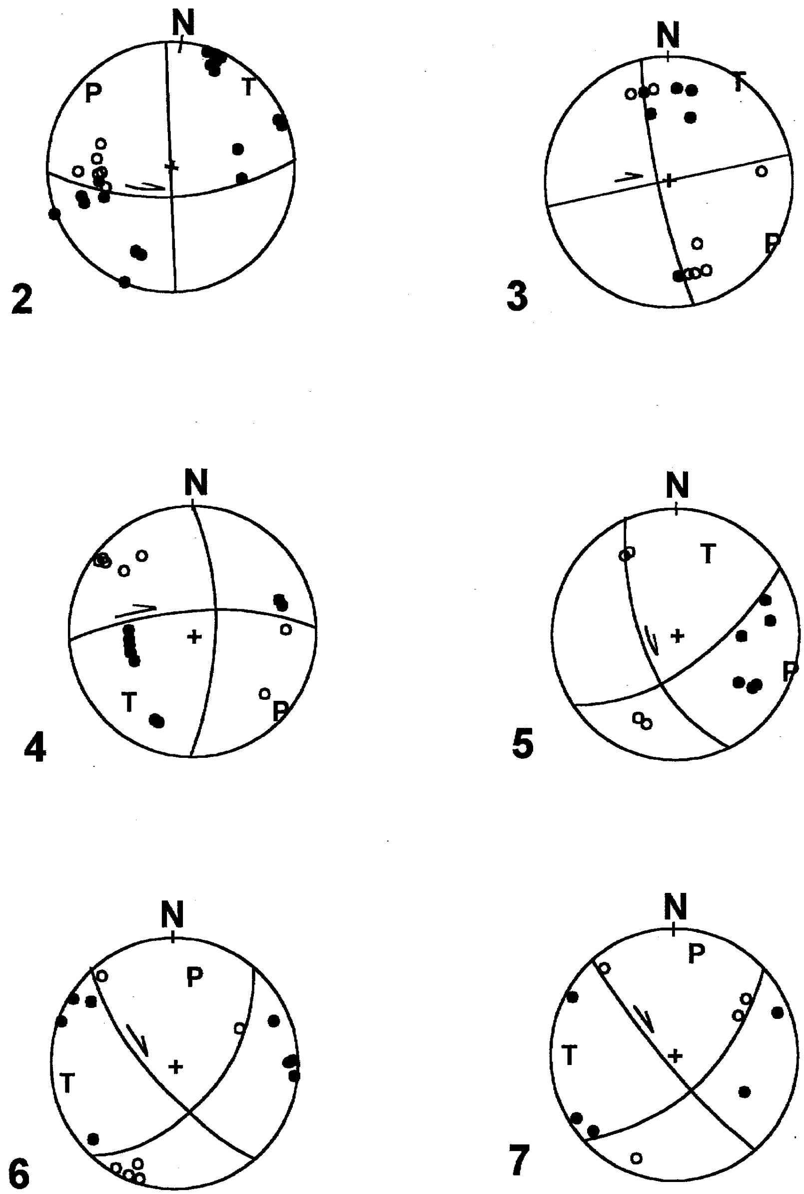

Figure 6. Composite focal mechanisms solutions for groups of events 2 to 7 in Figure 4 and Table 1. Description of symbols is identical to that in Figure 5.

Figure 4, and the same numbers are retained through Figures 4–7. We discuss below the results of this effort.

San Sebastián Fault Zone – SSF

Prior to our study, only one focal mechanism had ever been reported along this fault zone: That corresponding to the $M_s = 6.5$, Caracas earthquake of July 29th, 1967 (Rial, 1978), whose rupture occurred (Figure 2) NW of Caracas (Suárez and Nábêlek, 1990). The mechanism shows RLSS motion on an easterly oriented fault (Suárez and Nábêlek, 1990). Figure 4 shows two new composite focal mechanisms (CFM) along SSF (solutions 1 and 2). These solutions indicate RLSS motion on easterly-oriented vertical faults, essentially parallel to the SSF. Note that this fault zone in Figures 2–4 is not a simple linear structure but may be best characterized as a shear zone about 25 km wide. For these two

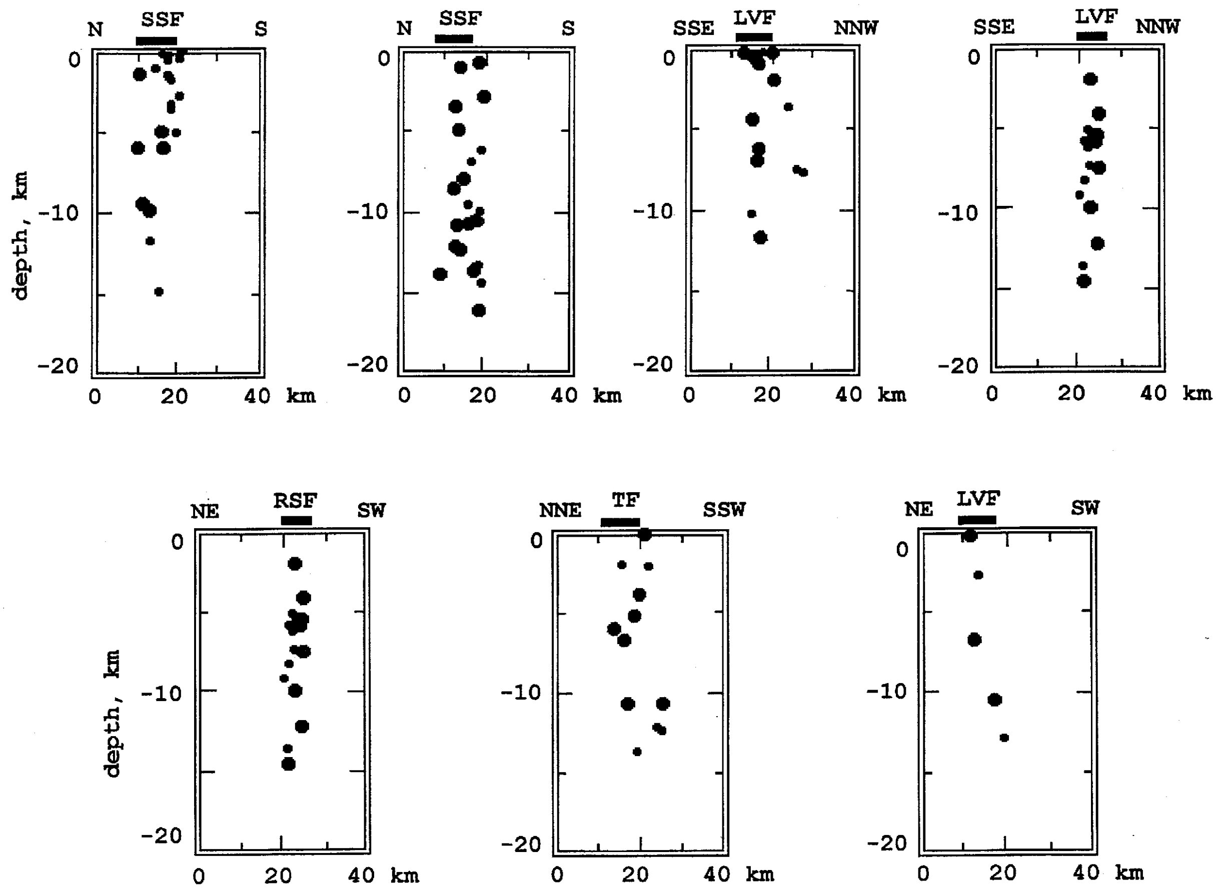

Figure 7. Vertical cross sections showing the focal-depth distribution (larger circles, $mb \geq 3$) for the groups of events nos. 1 to 7 in Figure 4. Smaller circles are events with mb in the range $2.5 \leq mb < 3$ located in the same corresponding region. Traces of fault zones are shown in the upper part of each profile. Faults: SSF: San Sebastián, LVF: La Victoria, TF: Tácata, RSF: right step faults where LVF is intercepted by Río Guárico fault (GF) in Figure 4. See text for explanations.

groups of events, the vertical cross sections (sections 1 and 2 in Figure 7) perpendicular to the strike of SSF strongly support the ocurrence of earthquakes on this fault zone. Both profiles define faults that, are almost vertical. It is noteworthy that in these and other profiles in Figure 7, the observed maximum depth does not exceed about ~ 15 km, a maximum depth limit similar to that observed for the San Andreas fault in California.

La Victoria Fault Zone – LVF

Figure 4 shows the first focal mechanisms ever reported along this fault zone. These composite solutions can be divided in two groups: one that indicates RLSS motion along easterly oriented fault planes (solutions 3 and 4); and another group that shows predominantly a combination of NW–SE striking RLSS motion and normal faulting (solutions 5 to 7). The former mechanisms are for shocks along the main trace of La Victoria fault (LVF). The latter mechanisms are for events located at or nearby sites where LVF is intercepted by NW-oriented subsidiary faults.

Corresponding vertical cross sections are displayed in Figure 7. Sections 3 and 4 are for solutions 3 and 4, respectively (we remind the reader that numerals are retained through Figures 4–7). These profiles, perpendicular to the strike of LVF, define near vertical fault planes. Thus, our observations are consistent with almost pure easterly-oriented RLSS along the main trace of La Victoria fault. Sections 5–7 are NE–SW profiles showing the focal depth distribution of events used to obtain mechanisms 5–7, respectively, at or nearby sites where LVF is intercepted by NW-oriented faults. These profiles define near vertical faults, consistent with the strike and dip of the NW-trending nodal plane indicated by their corresponding focal mechanism in Figure 4. Thus, in our interpretation, La Victoria fault is being offset (right stepping) at those places where it is intercepted by NW-trending faults, in an en-echelon like structural behavior that also includes a component of normal faulting at the interception sites. This structural behavior is also indicated by the neotectonic activity shown by a series of frequently offset morphological features along La Victoria fault zone (Schubert, 1986, 1988), including offset ridges and drainage, shutter ridges, fault scarps and steps, fault saddles and trenches, and alluvial terraces. This tendency appears to have a regional character: Pérez and Aggarwal (1981) point out (see their Figure 11) that the E–W oriented San Sebastián and El Pilar fault zones (SSF and PF in Figure 4) are part of the easterly trending Caribbean–South American plate boundary in north central Venezuela, with the SSF being offset (right stepping) south of Tortuga Island (TI in Figure 4) to become PF farther east.

It is possible that this segmentation of the main E–W faults is due to the existence of a bend in the main plate boundary, that changes from a nearly E–W strike in north-central Venezuela to a NE–SW trend along the Boconó fault in the west (Y. P. Aggarwal, personal communication, 1987; Suárez and Nábêlek, 1990); and to a NW–SE strike along Los Bajos-El Soldado fault zone farther east, in the Trinidad region (Figure 1; see Figure 11 of Pérez and Aggarwal, 1981). An alternate explanation could be that the strike-azimuth of the SSF and LVF fault zones (≤ 80) is larger than the azimuth of the Caribbean–South American slip vector (~ 75 °) (e.g., Deng and Sykes, 1995), which results in a transtensional component of deformation along those fault zones. As we will discuss below, this fault geometry somehow delimits the location and size of the largest events that could take place along them.

Other mechanisms

Finally, solutions 8 and 9 in Figure 4 (from Pérez et al., 1997), are for events on the NE-striking Boconó and NW-trending Morrocoy faults, respectively, in western Venezuela. These solutions indicate RLSS along those fault systems, which are part of a certainly multi-branched and complicated Caribbean-South American plate boundary in northwestern Venezuela and the southwestern Caribbean region (Dewey and Suárez, 1991; Deng and Sykes, 1995; Pérez et al., 1997). In northeastern Venezuela, Pérez and Aggarwal (1981) and Russo et al. (1993) report several composite fault plane solutions for microearthquakes associated to the easterly oriented El Pilar fault (PF). Their solutions show RLSS motion on nearly E–W oriented vertical faults.

Seismic moment release in North Central Venezuela (1983–1995)

Figure 8 shows the spatial distribution of seismic moment release in the study area from 1983 to mid-1995. This map was obtained by dividing the whole region into square cells with dimensions of [$\sim 25 \times 25$ km], and adding up the moments corresponding to every event with $m_b \geq 3$ that occurred within each cell, in the time span analyzed. The blank areas in Figure 8 correspond to regions where the seismic moment release calculated for each cell is less than 10^{15} Nm. The dotted and hatched areas correspond to regions where the seismic moment release is relatively high, in the range of 1 to 10×10^{15} Nm and 10 to 40×10^{15} Nm, respectively. The black cell corresponds to the $M_s = 6$ event that occurred in the region in 1989 and its aftershock sequence, with a moment of $\sim 10^{18}$ Nm.

The seismic moments for these events are calculated and listed by Mendoza and Pérez (1995; in preparation, 1997). A cut-off magnitude of $m_b = 3$ was used because the FUNVISIS earthquake catalog shows a constant rate of listing for the whole country for shocks with $m_b \geq 3$ since 1983 (Mendoza and Pérez, 1995). This, according to the results of several researchers (e.g., Habermann, 1982; Pérez, 1984; Pérez and Scholz, 1984), suggests that the catalog is largely complete for that magnitude range and time span. This also allows us to compare the seismic activity in a given region relative to another in the country, without introducing artifacts due to inhomogeneities in the catalog, e.g., man made changes in the seismicity rates of the type described by Habermann (1982, 1987), Pérez (1983, 1984) and Pérez and Scholz (1984, 1997). The moments were calculated from m_b according to the relation:

$$\mathrm{Log}(M_o) = (0.96 m_b \pm 0.08) + (18.19 \pm 0.16) \quad (1)$$

$$M_o, \mathrm{dyn-cm}; 2.3 \leq m_b < 6.$$

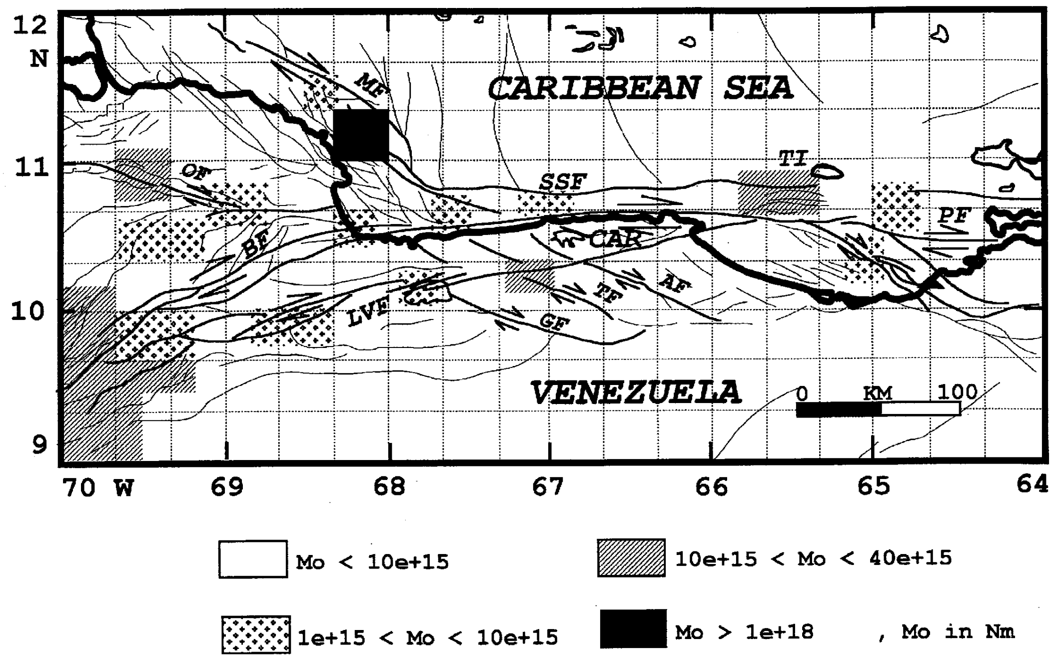

Figure 8. Spatial distribution of seismic moment released in north-central Venezuela from 1983 to mid 1995. Areas in blank correspond to regions releasing less than 10^{15} Nm. Dotted and hatched areas correspond to regions where the seismic moment released is relatively higher, in the range of 1–10 $\times$ 10^{15} Nm and 10–40 $\times$ 10^{15} Nm, respectively. The black cell corresponds to the $M_s = 6$ event that occurred in the region in 1989 and its aftershock sequence, with a moment of $\sim 10^{18}$ Nm. Note the absence of seismic moment release in the Caribbean Sea regions of north central Venezuela, and the existence of several places with relatively high moment release (dotted and hatched areas), when compared to other places (blank areas) in the region. See text for further explanations.

To get relation M_o was first obtained using the spectral analysis of *S* waves (Brune, 1970) for a series of events with m_b in the range $2.3 \leq m_b < 4.2$, digitally recorded by at least four seismological stations from 1990–1995; and moments reported by Archuleta et al. (1982) for earthquakes in the range $4 \leq m_b < 6$ in Mammoth Lakes, California.

It is clear that these seismic moments for the period 1983–1995, though accurate enough, are not representative of the long term seismic activity, and that they reflect only a small transient within the whole seismic cycle. The region, however, shows a very low background earthquake activity (Figure 2), and there is no homogeneous and sufficiently long-term earthquake catalog to be used for an in-depth seismological analysis. Bearing in mind these limitations, the following observations are made.

We first note in Figure 8 the absence of significant seismic moment release in the Caribbean sea regions of north-central Venezuela. Seismicity is constrained to occur in the southern regions of the San Sebastián fault zone (SSF), that is, in continental South America (see also the teleseismic locations for events with $m_b \geq 5$ from 1965–1995 in Figure 2), in general at depths $h \leq 15$ km (Figure 7). This suggests that SSF is the northernmost limit of the E–W oriented Caribbean-South America plate boundary in this region, and that south of it seismicity is occurring in the upper continental crust of the South American plate, in materials that are weaker than those forming the oceanic Caribbean plate (C. H. Scholz, personal communication, 1995). This phenomenon appears to be typical of transcurrent plate boundaries that put an oceanic plate into contact with a continental plate (Pérez and Sanz, unpublished data, 1995), like in California and the east coast of the Mediterranean Sea, i.e., San Andreas and Dead Sea faults.

Figure 8 also shows concentrations of seismic moment release at most of the fault crossing sites in the region. For instance, along La Victoria fault (LVF) there are areas of high moment release at its interception with the Boconó fault (BF) near 9.8° N; 69.7° W; and also at the sites where it is offset by the Río Guárico (GF) and Tácata faults (TF). Along San Sebastián fault

(SSF) there are areas of high moment release near its interception with the Morrocoy fault (MF); also southwest of Tortuga Island (TI), where it is intercepted and offset by RLSS faults; and at two sites northwest and north of Caracas, where it is intercepted by transverse faults occurring in both, the Caribbean floor and inland. Actually, these two latter sites were the nucleation and end of the 1967 rupture along SSF (see Figure 2). In our interpretation, these fault crossing or interception sites are just 'seismic barriers' subjected to high concentrations of stress. This results in a higher level of earthquake activity at those places along SSF and LVF, in comparison with other portions of these faults. In terms of the findings of Pérez and Scholz (1997), these barriers may mechanically control the location (nucleation and end) of future major seismic ruptures, as it was apparently the case during the 1967 Caracas earthquake.

Earthquake history and seismic potential of North Central Venezuela

Earthquake history

Figure 9 summarizes the location of the strongest shocks that have occurred in north central Venezuela since AD 1640, between the rupture zone of the March 26th, 1812 earthquake along the Boconó fault in the west, and the rupture zone of the 1766 event associated with the El Pilar fault in the east (Fielder, 1961; Kelleher et al., 1973; González and Rangel, 1973; Pérez, 1980). The magnitudes of these events are estimated to be in the range 7.5–8 (Grases, 1979; Pérez, 1980).

Two strong shocks have taken place (Figure 9) along San Sebastián fault zone (SSF) this century. On October 29th, 1900, a corrected $M_s = 7.6$ event (Pérez and Scholz, 1984; Pacheco and Sykes, 1992) ruptured large portions of this fault zone (Y. P. Aggarwal, unpublished data, 1987; see Figure 1 of Suárez and Nábêlek, 1990], causing strong damage along the coast and in Caracas itself. The size of this shock strongly suggests that the SSF plays a major role as part of the boundary between the Caribbean and the South American plate in this region. The other strong earthquake on SSF took place in 1967 ($M_w = 6.6$), rupturing a $\sim$50 km segment of this fault zone NW of Caracas (Suárez and Nábêlek, 1990). We pointed out above that the nucleation and end of the 1967 rupture occurred at seismic barriers where SSF is intercepted by transverse faults occurring in the Caribbean sea floor and inland.

Strong earthquakes have also taken place along La Victoria fault zone (LVF) in the past 350 years (Figure 9). Centeno-Grau (1940) and Grases (1980) report at least two damaging quakes associated to LVF, in 1641 and April 12th, 1878. Judging from their intensity reports, the 1641 event broke the portion of LVF in between the Río Guárico (GF) and Tácata (TF) faults, where Mercalli Intensities were as high as VIII. The magnitude of this event is estimated in the range of 6.4–7 (Y. P. Aggarwal, unpublished data, 1987; Suárez and Nábêlek, 1990). The shock in 1878, originally described by Ernst (1878), is of particular interest. The London *Times* (04–14–1878) reports a toll of 600 deaths and over £ 300,000 in damage. In Figure 9 we have assigned a Mercalli Intensity VIII–IX to those towns that, according to various Venezuelan and foreign newspapers of the time, were *totally destroyed* by that event. The sites are indicated by solid stars. These intensity values clearly suggest a $\sim$50 km break along La Victoria fault, southeast of Caracas. This rupture length corresponds to that of an event with a moment magnitude in the range of 6.5–7, similar to the 1967 Caracas earthquake.

Tectonic style and seismic potential

From the discussion above we conclude that moderate to large earthquakes have occurred in the past on both, San Sebastián (SSF) and La Victoria (LVF) fault zones, and that most of the Caribbean-South American plate motion is accommodated along this series of nearly E–W-oriented RLSS faults. This conclusion is supported by the occurrence of microseismicity and the nature of motion deduced above from fault plane solutions, along them. In our interpretation, the SSF is the main plate boundary, that is, the fault zone along which most of the relative plate motion is taken up during great earthquakes, like the one in 1900.

This style of seismic behavior in a transcurrent boundary that puts an oceanic and a continental plate into contact, in which there is a main fault (SSF) where great earthquakes occur, and secondary faults in the continental plate (e.g., LVF) generating moderate to large earthquakes during the seismic cycle, appears to be a phenomenon common to most of the boundaries of this type in the world. For instance, seismic activity ($m_b \geq 5$) in California along the segment of Pacific-North American plate boundary associated with the 1906 great rupture, has mostly taken place in the con-

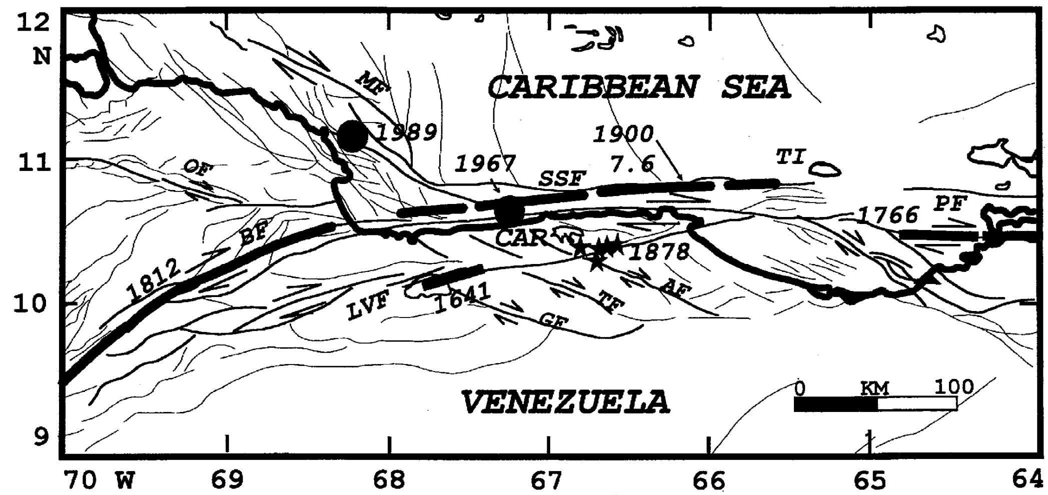

Figure 9. Strongest earthquakes occurred in north-central Venezuela since AD 1640. Thick lines indicate extend of ruptures. Numerals indicate year of occurrence. The surface-wave magnitude for the 1900 event on San Sebastián fault (7.6) is indicated. Large ruptures in 1766, 1900 and 1812 are from Y. P. Aggarwal, unpublished data, (1987), published by Suárez and Nabêlek (1990). Closed circles are the main epicenters of the 1967 ($M_s = 6.5$) and 1989 ($M_s = 6$) events. Stars are intensities VIII to IX assigned in this study to those places where towns are reported to have been totally destroyed during the 1878 earthquake. Other symbols as in Figure 2. See text for explanations.

tinental North American plate both, before and after the 1906 event, that is, during the seismic cycle. No activity has taken place in the oceanic Pacific plate (see, e.g. Ellsworth, et al., 1981; Pérez 1983; Sykes and Jaumé, 1990). Also note that in this region, the San Andreas fault takes up about a half of the Pacific-North American relative plate motion, whereas the other half is distributed along other RLSS subsidiary faults (e.g., Herd, 1979; Ellsworth et al., 1981).

A similar case may be occurring in north-central Venezuela and southern Caribbean. The fault system conformed by the main traces of the Boconó, San Sebastián and El Pilar faults (Figure 1) appears to be moving at a rate of ~ 10 mm/y (Schubert and Sifontes, 1970; Pérez and Aggarwal, 1981; Schubert, 1984; Y. P. Aggarwal, unpublished data, 1987), whereas the full rate of motion along the entire fault zones (70–100 km wide) is on the order of 20 mm/y or more (Dewey and Suárez, 1991; Deng and Sykes, 1995; Pérez et al., 1997). Thus, about a half of the Caribbean-South American plate motion in north central Venezuela may be taken up along San Sebastián fault, whereas the other half may be distributed along other E–W oriented RLSS subsidiary faults, like La Victoria fault zone. Schubert (1984, 1986, 1988) reports firm geological evidence of significant (2 to 3 mm/y) RLSS motion on the main trace of this fault during Pleistocene and Holocene times. Note also in Figure 2 that the San Sebastián fault zone is composed of at least two nearly parallel faults along the coast (Beltrán, 1993). It is clear that new Global Positioning System (GPS) measurements are necessary in the region to help resolve all these uncertainties.

Nevertheless, from the discussion above we conclude that the repeat time of the $M_s = 7.6$, 1900 event on San Sebastián fault is on the order of ~ 250 years, if one is to expect ~ 2.5 meters of displacement during a break of that size (e.g., Sykes and Quitmeyer, 1981), and assuming a rate of motion of ~ 10 mm/y along the main trace of this fault. This suggests that the region may be relatively far from a repeat of this event. It does not mean, however, that destructive shocks will not occur in the area during the intervening period. Indeed, we demonstrated the occurrence of moderate to large events in the times before the 1900 quake. Also, moderate shocks occurred in north-central Venezuela (Figure 9) in 1967 ($M_w = 6.6$) causing extensive damage to Caracas, and in 1989 ($M_s = 6$). Thus, it is feasible that other strong shocks may occur in the region before the repeat of the 1900 event, particularly along segments of the seismically active faults we have identified in this study. These include La Victoria fault, and the NW–SE-oriented ones that occur in the region, among them those to the west of Caracas. In the context of the findings of Pérez (1983) and Pérez and Scholz (1997), the fault crossing or interception sites, – ‘barriers' – that we have identified in the region, are likely to control the size, nucleation and ends of such a ruptures, as it was the case during the 1967 Caracas earthquake and many other events in the world reported by the latter authors. We hope further seismological and GPS studies will lead to a better understanding of the present day tectonics and seismic potential in this region.

Acknowledgments

We thank the students of Simón Bolívar University's seismology group for their help in data analysis and Jorge Mendoza for his help in the computational parts of this research. Conversations with Alirio Bellizzia and Luis Urbina were stimulating. The revised microearthquake catalog used in this investigation is available from the authors upon request. Simón Bolívar University contribution number USB-CT97-04.

References

Archuleta, R. J., Cranswick, E., Mueller, C., and Spudich, P., 1982, Source parameters of the Mammoth Lakes, California, earthquake sequence, *J. Geophys. Res.*, **87**, 4595–4607.

Beltrán, C., 1993, *Neotectonic Map of Venezuela*, scale 1:2 000 000, Venezuelan Foundation for Seismological Research FUNVISIS, Caracas, Venezuela.

Bellizzia, A., Pimentel, N., and Bajo, R., 1976, Structural Geology map of Venezuela, scale 1:500 000, Ministry of Energy and Mines, Caracas, Venezuela.

Brune, J. N., 1970, Tectonic stress and the spectra of seismic shear waves from earthquakes, *J. Geophys. Res.*, **75**, 4997–5009. (Correction: idem., 1971, *J. Geophys. Res.*, **76**, 5002).

Burke, K. C., Cooper, C., Dewey, J. F., Mann, P., and Pindell, J. L., 1984, Caribbean tectonics and relative motions, *Mem. Geol. Soc. Am.*, **162**, 31–63.

Centeno-Grau, M., 1940, *Seismological Studies* (in Spanish), 300 pp., Litografía del Comercio, Caracas, Venezuela.

Deng, J., and Sykes, L. R., 1995, Determination of Euler pole for contemporary relative motion of Caribbean and North American plates using slip vectors of interplate earthquakes, *Tectonics*, **14**, 39–53.

Dewey, J. W., and Suárez, G., 1991, Seismotectonics of Middle America. In Slemmons, D. B., Engahl, E. R., Zovak, M. D., and Blackwell, D. (eds), *Neotectonics of North America*, Geological Society of America, Boulder, Colo., pp. 309–321.

Ellsworth, W. L., Lindh, A. G., Prescott, W. H., and Herd, D. G., 1981, The 1906 San Francisco earthquake and the earthquake cycle. In Simpsom, D. W., and Richards, P. G. (eds), AGU, *Earthquake Prediction, An International Review*, Maurice Ewing Series 4, Washington D.C., pp. 126–140.

Ernst, A., 1878, Earthquake in Venezuela, *Nature*, **18**, 130.

Fielder, G., 1961, Areas affected by earthquakes in Venezuela (in Spanish), *Venez. Geol. Conf. Bol. Geol.*, **4**, 1791–1810.

González, C. L., and Rangel, R., 1979, Epicentral intensities during historical earthquakes in the Caribbean (in Spanish), B.Sc. thesis, Central Univ., Caracas, Venezuela, 101 pp.

Grases, J., 1979, Destructive earthquakes in eastern Venezuela, Orinoco Delta and adjacent regions (in Spanish), *Technical Report*, INTEVEP, Caracas, Venezuela.

Grases, J., 1980, Investigation on the destructive earthquakes that have affected central and western Venezuela, 3 Vols., *Technical Report*, INTEVEP, Caracas, Venezuela.

Habermann, R. E., 1982, Consistency of teleseismic reporting since 1963, *Bull. Seism. Soc. Am.*, **72**, 93–111.

Habermann, R. E., 1987, Man-made changes of seismicity rates, *Bull. Seism. Soc. Am.*, **77**, 141–159.

Herd, D. G., 1979, Neotectonic framework of central coastal California and its implications to microzonation of the San Francisco Region. In Brabb, E. E. (ed.), *Progress on Seismic Zonation in the San Francisco Bay Region*, U.S. Geol. Surv. Circ., No. 807, 3–12.

Jordan, T. H., 1975, The present-day motion of the Caribbean plate, *J. Geophys. Res.*, **80**, 4433–4439.

Kelleher, J. A., Sykes, L. R., and Oliver, J., 1973, Possible criteria for predicting earthquake locations and their application to major plate boundaries of the Pacific and the Caribbean, *J. Geophys. Res.* **78**, 2547–2585

Mendoza J., and Morgan, D., 1985, BASIC-HYPO: a BASIC language hypocenter location program, *Bull. Seism. Soc. Am.* **75**, 1211–1216

Mendoza J., and Pérez, O. J., 1995, Seismic moment catalog of shallow earthquakes in Venezuela, 1900–1993 (abstract), *Acta Científica Venezolana, Trans. XLV Convención ASOVAC*, **46** (suppl.), 290.

Minster, J. B., and Jordan, T. H., 1978, Present-day plate motions, *J. Geophys. Res.* **83**, 5331–5354.

Molnar P., and Sykes, L. R., 1969, Tectonics of the Caribbean and Middle America regions from focal mechanisms and seismicity, *Geol. Soc. Am. Bull.* **80**, 1639–1684.

Pacheco J. F., and Sykes, L. R., 1992, Seismic moment catalog of large earthquakes, 1990 to 1989, *Bull. Seism. Soc. Am.*, **82**, 1306–1349.

Pérez, O. J., 1980, Microseismicity and tectonics of northeastern Venezuela (in Spanish), *Technical Report*, *INTEVEP*, Caracas, Venezuela.

Pérez, O. J., 1983, Spatial-temporal energy characteristics of seismicity occurring during the seismic cycle: A reappraisal, Ph.D. thesis, Columbia University, N.Y., 129 pp.

Pérez, O. J., 1984, Lack of uniformity of instrumental data on strong earthquakes in seismic catalogs (1904–1980), *Izv. Acad. Sci. USSR, Phys. Solid Earth* **20**, 721–729.

Pérez, O. J., and Aggarwal, Y. P., 1981, Present-day tectonics of the southeastern Caribbean and northeastern Venezuela, *J. Geophys. Res.* **86**, 791–804.

Pérez, O. J., and Scholz, C. H., 1984, Heterogeneities of the instrumental seismicity catalogue (1904–1980) for strong shallow earthquakes, *Bull. Seism. Soc. Am.* **74**, 669–686.

Pérez, O. J., and Scholz, C. H., 1997. Long term seismic behavior of the focal and adjacent regions of great earthquakes during the time between two successive shocks, *J. Geophys. Res.* **102**, 82-3–8216.

Pérez, O. J., Jaimes, M. A., and Garciacaro, E., 1997, Microseismicity evidence for subduction of the Caribbean beneath the South American Plate in Northwestern Venezuela, *J. Geophys. Res* (in press).

Rial, J. A., 1978, The Caracas, Venezuela, earthquake of July 1967: A multiple source event, *J. Geophys. Res.* **83**, 5405–5414.

Rod, E., 1956, Strike slip faults of northern Venezuela, *Am. Assoc. Petr. Geol. Bull.* **40**, 457–476.

Russo, R. M., Speed, R. C., Okal, E. A., Shepherd, J. B., and Rowley, K. C., 1993, Seismicity and tectonics of the Southeastern Caribbean, *J. Geophys. Res.* **98**, 299–319.

Schubert, C., 1981, Are the Venezuelan fault systems part of the southern Caribbean plate boundary? *Geol. Rundsch.* **70**, 542–551.

Schubert, C., 1984, Basin formation along the Boconó-Morón -El Pilar fault system, Venezuela, *J. Geophys. Res.* **89**, 5711–5718.

Schubert, C., 1986, Neotectonic aspects of La Victoria fault zone and origin of the Santa Lucía-Ocumare del Tuy Basin, Venezuela (in Spanish), *Acta Científica Venezolana* **37**, 278–286.

Schubert, C., 1988, Neotectonics of La Victoria fault zone, north-central Venezuela, *Annales Tectonicae* **2**, 58–66.

Schubert, C., and Sifontes, R. S., 1970, Boconó fault, Venezuelan Andes: Evidence of post-glacial movement, *Science* **170**, 66–69.

Suárez, G., and Nábêlek, J., 1990, The 1967 Caracas earthquake: Fault geometry, direction of rupture propagation, and seismotectonics implications, *J. Geophys. Res.* **95**, 459–474.

Sykes, L. R., and Ewing, M., 1965, The seismicity of the Caribbean region, *J. Geophys. Res.* **70**, 5065–5074.

Sykes, L. R., and Jaumé, S. C., 1990, Seismic activity on neighbouring faults as a long-term precursor to large earthquakes in the San Francisco Bay area, *Nature* **348**, 595–599.

Sykes, L. R., and Quitmeyer, R. C., 1981, Repeat times of great earthquakes along simple plate boundaries. In Simpsom, D. W., and Richards, P. G. (eds), *Earthquake Prediction, An International Review*. Maurice Ewing Series **4**, 217–247.